PROCEEDINGS OF SPIE

SPIEDigitalLibrary.org/conference-proceedings-of-spie

Insulation properties of 3D-printed components for use in interior building panels

Amatullah Kose, Indika Perera, Nadarajah Narendran, Jean Paul Freyssinier, Farjana Mostafa

Amatullah Kose, Indika Perera, Nadarajah Narendran, Jean Paul Freyssinier, Farjana Mostafa, "Insulation properties of 3D-printed components for use in interior building panels," Proc. SPIE 12670, 3D Printing for Lighting, 1267008 (29 September 2023); doi: 10.1117/12.2676863

SPIE.

Event: SPIE Optical Engineering + Applications, 2023, San Diego, California, United States

Insulation properties of 3D-printed components for use in interior building panels

Amatullah Kose [a], Indika Perera [a], Nadarajah Narendran* [a], Jean Paul Freyssinier [a], and Farjana Mostafa[a]

[a]Lighting Research Center, Rensselaer Polytechnic Institute, 21 Union St., Troy, NY 12180, USA

ABSTRACT

This study characterized the thermal conductivity (κ) values of a few commonly available fused-filament fabrication (FFF) type 3D printing materials that have the potential to be used to 3D-print interior architectural wall panels. The materials included polylactic acid (PLA), acrylonitrile butadiene styrene (ABS), and polyethylene terephthalate glycol (PETG). Three infill percentages (20, 60, and 98%) and three infill patterns (grid, zigzag, and honeycomb) were investigated in the study. The characterized thermal conductivity values revealed that these 3D-printed material sample coupon thermal conductivity values ranged from 0.15 to 0.31 W m^{-1} K^{-1} and were comparable to gypsum plaster, drywall, and hardwood. Generally, lower infill densities (e.g., infill percentage ~20%) contributed to sample coupons with lower thermal conductivity values (e.g., κ~0.15 W m^{-1} K^{-1}). Zigzag and honeycomb infill patterns generally showed lower thermal conductivity values (~30 to 60% lower κ-value) than grid-type infill patterns for a given infill density. 3D-printed sample coupons with PLA material indicated higher thermal conductivity values (~10-33% higher κ-value) when compared to ABS and PETG 3D-printed sample coupons. The study results also showed that 3D printing could fabricate components such as interior building panels with desired target thermal conductivity values. The findings also showed that by selecting the combination of 1) material, 2) infill pattern, and 3) infill percentage, constant or localized gradient thermal conductivity values could be engineered that are difficult to achieve with traditional interior building materials.

Keywords: 3D printing, additive manufacturing, fused-filament fabrication, thermal conductivity, polymer material, building interior, architecture, insulation material

1. INTRODUCTION

Digital technologies and related innovations continue to impact all aspects of modern life, including architecture and construction.[1] 3D printing is one such technology gaining increasing interest in the Architecture, Engineering, and Construction (AEC) industry because of its potential to revolutionize existing building practices and materials used. News items about 3D-printed homes and buildings are now commonplace and represent the increasing interest in research and development of 3D printing for the built environment.[2],[3] At present, research remains focused on the printability and structural capacity of the 3D-printed build.[4]

It has been estimated that the envelope accounts for up to 60% of the heat gain or loss in typical buildings.[5] This directly impacts the energy efficiency and comfort of the indoor environment. One critical aspect of a building's envelope is the choice and design of the insulation used in the interior of the architectural space. The thermal conductivity of traditional building construction material ranges from 0.04 W m^{-1} K^{-1} (organic-bonded glass fiber in board and slab form) to 1.3 W m^{-1} K^{-1} (masonry brick), with most materials having a thermal conductivity values ~0.1-0.5 W m^{-1} K^{-1}.[6]

*Corresponding author: Nadarajah Narendran
E-mail: narenn2@rpi.edu; Telephone: +1 (518) 276-7176; Website: https://www.lrc.rpi.edu/programs/solidstate/

3D Printing for Lighting, edited by Nadarajah Narendran, Govi Rao,
Proc. of SPIE Vol. 12670, 1267008 · © 2023 SPIE
0277-786X · doi: 10.1117/12.2676863

At Rensselaer's Lighting Research Center (LRC), researchers are developing a 3D-printed building interior wallboard concept that integrates lighting, electrical connectivity, sensors, and communication devices. These functions are in addition to the mechanical, thermal, acoustic, and surface texture properties that can be optimized for different building interior needs.[7] The overarching value of this concept is the optimization of building materials system integration that is expected to increase design, construction, and energy efficiency in residential and commercial buildings.[8]

Therefore, characterizing and analyzing the fundamental properties, such as thermal conductivity, of 3D-printed components is essential to understanding their performance in potential architectural and construction applications. Past literature with polymer 3D printing material has reported an increase in infill percentage increased thermal conductivity,[9],[10] and the infill patterns that create smaller volumes of material voids increased thermal conductivity.[9]

Therefore, the objectives of the study were to identify the insulative properties of 3D-printed components related to (1) material, (2) infill percentage, and (3) infill pattern for potential building interior panel applications. It is important to recognize that although many characteristics are critical in selecting insulation materials, including their hygroscopic, acoustic, fire retardation, environmental impact during manufacturing and at the end of life, and cost, this study focuses on the thermal insulating properties only. Specifically, this project aims to compare the potential thermal insulating capabilities of 3D-printable materials to those of traditional materials.

2. METHODOLOGY

2.1 3D printing of the sample coupons

A commercial computer-aided designing (CAD) software package was used to design sample coupons of 19 mm diameter disc-shapes in thicknesses of 1.0, 2.5, and 4.0 mm. The modeled CAD files were exported as .stl files. The .stl files were sliced at three infill patterns (grid, zigzag, and honeycomb as shown in Figure 1), at three infill percentages (20, 60, and 98%), at a 0.2 mm layer height for a 0.75 mm nozzle orifice on a modified MakerGear M2 dual-extruder using Simplify3D® commercial slicing software version 4.1.2. The sliced CAD models were then 3D-printed using commercially available generic polylactic acid (PLA), acrylonitrile butadiene styrene (ABS), and polyethylene terephthalate glycol (PETG) filaments of 1.75 mm nominal diameter. The 3D-printed sample coupons were lightly polished on the top and the bottom surfaces with 400-grit sandpaper to maintain surface roughness. Figure 1 shows 45 of the 3D-printed sample coupons in (a) PLA grid, (b) PLA zigzag, (c) PLA honeycomb, and (d) PETG grid and ABS grid. The 3D-printed and polished sample coupons were measured to have diameters of 18.9±0.2 mm and thicknesses of 1.1±0.2, 2.6±0.2, and 4.1±0.2 mm.

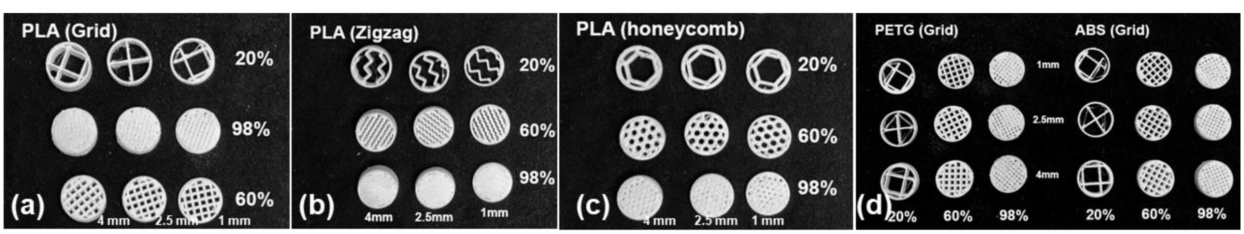

Figure 1. 3D-printed sample coupons

2.2 Thermal conductivity characterization experiment apparatus

The thermal conductivity characterization of the 3D-printed sample coupons was tested using a custom experimental apparatus similar to that described in the ASTM C518 and ASTM C177 standards.[11],[12] The authors used a redesigned version of the apparatus used by Terentyeva et al. (2019)[13] in the current study for characterizing the 3D-printed sample coupons (Figure 2).

The setup on the top of the stack has a resistive heating element fixed to an aluminum disc with an embedded thermocouple. Another aluminum disc with embedded thermocouples is mounted on a heat sink. The sample coupon under test of unknown thermal conductivity is sandwiched between these two aluminum hot and cold blocks, and a paste-type thermal interface material is used to provide good thermal contact between the aluminum discs and the sample coupon under test. A mechanical screw-type clamping mechanism was used on the hot end side to maintain a repeatable contact pressure. Insulation was used to reduce the thermal losses to the ambient, forcing the heat to transfer from the hot end to the cold plate through the test sample coupon. Three thicknesses of the test sample coupons of the same material and print parameter combinations are used to determine the thermal conductivity of interest. The electrical power supply and the thermocouple data acquisition system are not illustrated in Figure 2. The characterization experimental setup was used to measure each of the sample coupons.

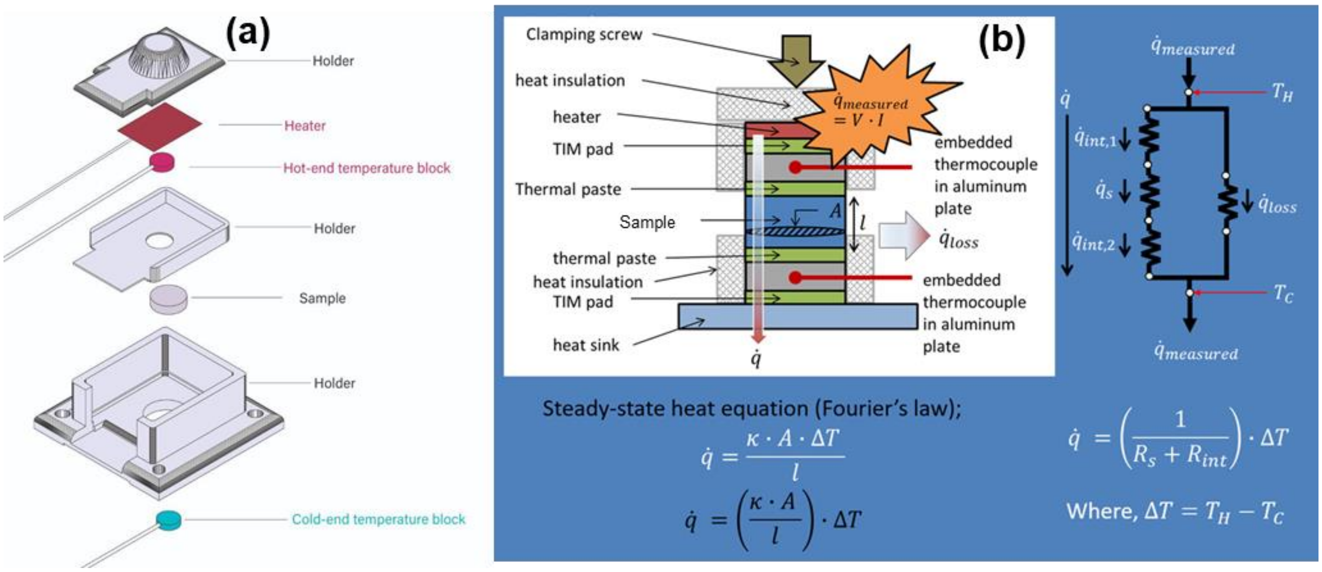

Figure 2. (a) Schematic diagram of the experiment apparatus and (b) Schematic diagram of parallel thermal resistance approach to thermal conductivity calculations

2.3 3D printed sample coupon characterization

To calculate the thermal conductivity of a single combination of 1) material, 2) infill pattern, and 3) infill percentage, sample coupons of three thicknesses were used similar to past literature.[13] Each sample coupon was subjected to five heat settings by varying the electrical voltage and current applied to the heating element, letting the temperature on both temperature measurement blocks reach the steady-state operation while maintaining the electrical power input at the desired value to the heating element. The subsequent calculations related to the thermal conductivity estimate are also described in past literature.[13]

Using Fourier's law for heat transfer (Equation 1) via heat conduction through a sample coupon:

$$\dot{q} = \frac{\kappa \cdot A \cdot \Delta T}{l} \quad \text{Eq. 1}$$

where, $\dot{q}$ is the steady-state rate of heat transfer, κ is the isotropic bulk thermal conductivity of the medium, A is the cross-sectional area of heat transfer, ΔT is the temperature differential driving the heat transfer, and l is the distance between the locations where the ΔT is measured. $\dot{q}/\Delta T$ was calculated from the measurements of the power applied to the heater and the temperature gradient measured by the thermocouples. A calibration of the test apparatus was conducted to quantify the heat loss ($\dot{q}_{loss}$) in Figure 2 (b) that is dissipated to the ambient without conducting through the sample coupon using reference samples of known thermal conductivity. Then, using the thermal resistance definition (Equation 2) and parallel thermal resistance network model illustrated in Figure 2 (b), the sample coupon thermal resistances were calculated using Equation 3.

$$\frac{1}{R_{measured}} = \dot{q}/\Delta T = \frac{1}{R_{losses}} + \frac{1}{R_{sample}} \quad \text{Eq. 2}$$

$$R_{sample} = \frac{l}{\kappa \cdot A} = \left(\frac{1}{R_{measured}} - \frac{1}{R_{losses}}\right)^{-1} \quad \text{Eq. 3}$$

Then $\left(\frac{1}{R_{measured}} - \frac{1}{R_{losses}}\right)^{-1}$ was plotted against l for the three different thicknesses of sample coupons from the same material, infill pattern, and infill percentage combination (Figure 3). The thermal conductivity value was calculated by dividing the inverse slope of the line of best fit through the data points by the average surface area (A) of the sample coupons.

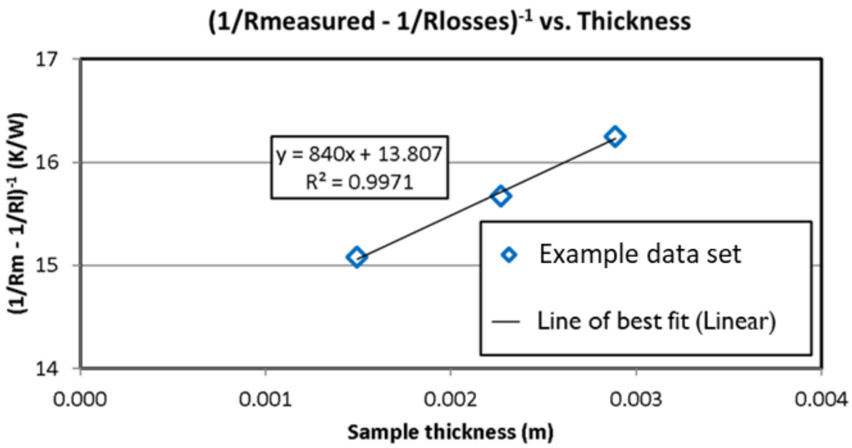

Figure 3. Example of thermal conductivity calculation from three thicknesses of sample coupons 3D-printed with the same combination of material, infill pattern, and infill percentage.

3. RESULTS

In order to characterize the insulative properties of the 3D-printed sample coupons, the study used thermal conductivity estimates using the above-described, in-house developed and calibrated, steady-state thermal conductivity measurement apparatus and the calculation method. The calibration of the thermal conductivity apparatus showed the experimental uncertainty in the characterized thermal conductivity was <0.043 W m^{-1} K^{-1} with an experiment relative uncertainty of ≤14%.

Figure 4 illustrates the characterized thermal conductivity values of sample coupons 3D-printed with PLA, ABS, and PETG materials in the grid infill pattern. Hardwood, drywall, and gypsum plaster thermal conductivity values from the literature[6] are also plotted for comparison. The error bars represent the standard deviation of the characterized thermal conductivity value from three repeated sets of measurements of the 3D-printed sample coupons. The general trend of increase in infill percentage increases the thermal conductivity of the 3D-printed sample coupon was observed. This is similar to other literature that has observed the same effect of increasing infill percentage causing an increase in the thermal conductivity values of 3D-printed components.[9],[10] The 3D-printed PLA sample coupons consistently showed a higher thermal conductivity, ~10-33% higher κ-value compared to ABS and PETG sample coupons as the infill percentage was increased, indicating a higher bulk thermal conductivity value of PLA.

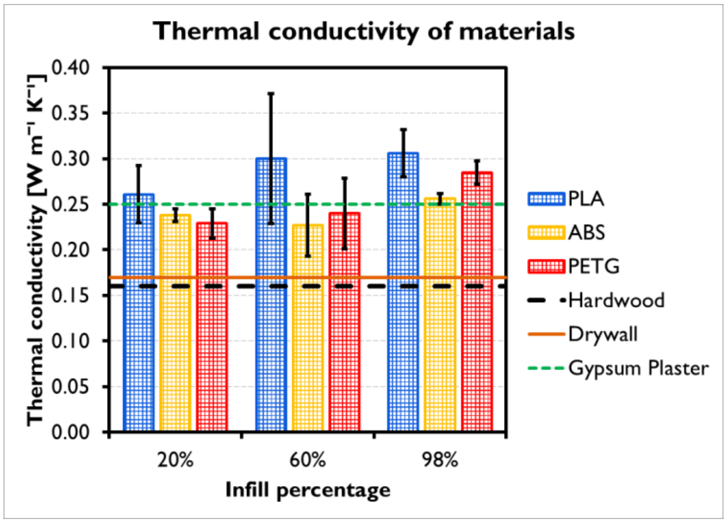

Figure 4. Characterized thermal conductivity values of 3D-printed sample coupons in PLA, ABS, and PETG materials.

Figure 5 shows the thermal conductivity of 3D-printed PLA sample coupons in three infill patterns: grid, zigzag, and honeycomb. The common trend of increasing infill percentage leading to an increase in the thermal conductivity of the 3D-printed components was also observed here, confirming the previous findings of the study and past literature.[9],[10] Additionally, Figure 5 illustrates even at the same infill percentage, with different infill patterns, the thermal conductivity of the 3D-printed sample coupons can be changed to have the desired target thermal performance. As an example, gypsum plaster thermal performance with respect to thermal conductivity can be achieved by employing a grid pattern at 20% infill percentage while at the same infill percentage of 20%, by 3D-printing the sample with a zigzag infill pattern, a thermal conductivity value close to drywall or hardwood can be achieved.

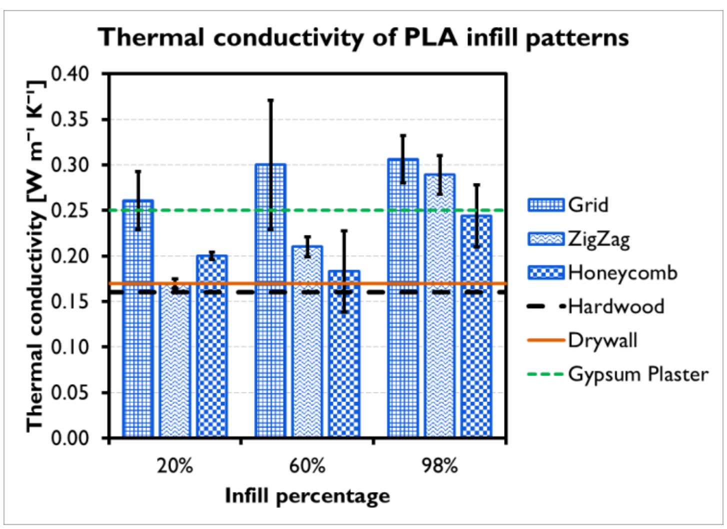

Figure 5. Characterized thermal conductivity values of 3D-printed PLA sample coupons in grid, zigzag, and honeycomb infill patterns.

Zigzag and honeycomb infill patterns generally showed lower thermal conductivity values (~30 to 60% lower κ-value) than grid-type infill patterns for a given infill percentage. Past literature attributes this to the creation of circular flows in the cavities created by the different infill patterns of the 3D-printed component.[9] This can also be visualized in the relatively larger void spaces in the zigzag 20% infill percentage (Figure 1 (b) top-row) compared to the 20% infill percentage grid (Figure 1 (a) top-row) and honeycomb (Figure 1 (c)top-row). As the infill percentage is increased from 20% to 60% and 90%, the zigzag infill pattern almost turns into a line with minimal scalloping (Figure 1 (b)) decrease in the relative size of the void spaces, reducing the size of the convection circular flow path and thereby increasing the thermal conductivity.[9]

4. SUMMARY

This paper presented insulative property characterizations based on material, infill pattern, and infill densities of 3D-printed sample coupons for building interior panel applications. The insulative properties of the 3D-printed sample coupons were characterized by estimating thermal conductivity using an in-house developed and calibrated steady-state thermal conductivity measurement apparatus. The calibration of the thermal conductivity apparatus showed the experimental uncertainty in the characterized thermal conductivity was <0.043 W m^{-1} K^{-1} (experiment relative uncertainty ≤14%).

PLA, ABS, and PETG commercially available filament materials were used to 3D print 19 mm diameter disc-shaped sample coupons in three heights of 1.0, 2.5, and 4.0 mm with fused-filament fabrication 3D printers at a 0.2 mm layer height. Each combination of material and height of disc variant sample coupon was 3D–printed in three infill patterns: grid, zigzag, and honeycomb, and three infill densities: 20%, 60%, and 98%.

The characterized thermal conductivity values revealed that these 3D-printed material sample coupon thermal conductivity values ranged from 0.15 to 0.31 W m^{-1} K^{-1} and were comparable to gypsum plaster, drywall, and hardwood. Generally, lower infill densities (e.g., 20% infill density compared to 60% and 98% infill densities) contributed to sample coupons with lower thermal conductivity values. Zigzag and honeycomb infill patterns generally showed lower thermal conductivity than grid-type infill patterns for a given infill density. 3D-printed sample coupons with PLA material indicated higher thermal conductivity values when compared to ABS and PETG 3D-printed sample coupons.

The study results also showed that 3D printing could create interior building panels with desired target thermal conductivity values by selecting material, infill pattern, and infill density parameters with either constant or localized gradient properties that are difficult to achieve with traditional interior building materials.

ACKNOWLEDGMENTS

The authors would like to acknowledge the financial support of the New York State Energy Research and Development Authority (NYSERDA) under NYSERDA Agreement 173123 and the NYSERDA Project Manager, Joseph Borowiec, for his support. The authors would like to iterate that such support does not constitute an endorsement by NYSERDA of the views expressed herein. The authors also gratefully appreciate Jennifer Taylor from the Lighting Research Center (LRC) for her help in preparing this manuscript. The authors are also thankful to Kyle Funk and Bryan Bauer of the LRC for their assistance and effort in setting up the characterization apparatus and the data acquisition systems.

REFERENCES

[1] Hamidi, F., and A. Farhad, "Additive manufacturing of cementitious composites: Materials, methods, potentials, and challenges." Construction and Building Materials 218 (2019): 582-609.

[2] The first 3D-printed housing community in the US is being built in the California desert. https://www.cnn.com/2021/03/18/business/california-3d-printed-neighborhood-trnd/index.html

[3] ICON builds 3D-printed houses from disaster-proof concrete in Texas. https://www.dezeen.com/2021/03/16/icon-3d-printed-houses-austin-texas/

[4] Pessoa, S., A.S. Guimarães, S.S. Lucas, and N. Simões, 2021. "3D printing in the construction industry – A systematic review of the thermal performance in buildings," Renewable and Sustainable Energy Reviews, 141.

[5] Kumar, D., M. Alam, P.X. Zou, J.G. Sanjayan, and R.A. Memon, "Comparative analysis of building insulation material properties and performance." Renewable and Sustainable Energy Reviews, 131. (2020).

[6] Incropera, F.P., D.P. DeWitt, T.L. Bregman, and A.S. Lavine, Introduction to Heat Transfer, 6th Edition, John Wiley and Sons, 2006. Table A.3

[7] Lighting Research Center. 3D Printing for Lighting News. https://www.lrc.rpi.edu/programs/solidstate/news/3DInteriorWall.asp

[8] Narendran, N., Perera, I., and Freyssinier, J.P. 2021. Rensselaer Polytechnic Institute. Provisional U.S. Patent Application No.: 63/193,645, 3D-Printed Building Material System.

[9] Grabowska, B., and J. Kasperski, "The Thermal Conductivity of 3D Printed Plastic Insulation Materials – The Effect of Optimizing the Regular Structure of Closures." Materials 13(19):4400. (2020). doi: 10.3390/ma13194400

[10] Sonsalla, T., A.L. Moore, W.J. Meng, A.D. Radadia, L. Weiss, "3-D printer settings effects on the thermal conductivity of acrylonitrile butadiene styrene (ABS)," Polymer Testing, 70, (2018) pp. 389-395. doi: 10.1016/j.polymertesting.2018.07.018

[11] ASTM C518–17: Standard Test Method for Steady-State Thermal Transmission Properties by Means of the Heat Flow Meter Apparatus.

[12] ASTM C177–19: Standard Test Method for Steady-State Heat Flux Measurements and Thermal Transmission Properties by Means of the Guarded-Hot-Plate Apparatus.

[13] Terentyeva, V., I.U. Perera, and N. Narendran, "Analyzing theoretical models for predicting thermal conductivity of composite materials for LED heat sink applications," Proceedings of the IES 2017 Annual Conference, Aug. 10-12, Oregon.